TITLE: LARGE AREA SMART PIEZOELECTRIC AND PYROELECTRIC SENSORS

Contract: DAJA 45-93-C-0017
(R & D 6980-EE-01)

NINTH INTERIM REPORT

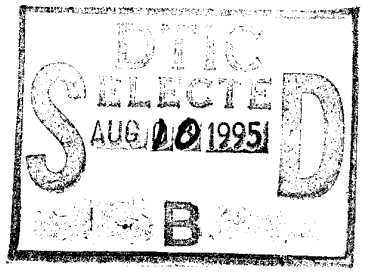

D.K. Das-Gupta & M.P. Wenger
School of Electronic Engineering and Computer Systems
University of Wales, Bangor
Dean Street
Bangor, Gwynedd, LL57 1UT, U.K.

Telephone: (01248) 382696
Fax: (01248) 361429
Email dilip@uk.ac.bangor.sees

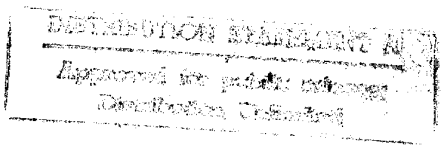

July, 1995

Introduction

In the eighth interim report investigation into the viability of transducers made from composite materials for use as acoustic emission detectors was made. The report showed that the transducers were capable of detecting acoustic emission from a pencil lead break and an attempt was made to characterise the frequency response of the various transducers over the range 0 - 1MHz by use of the face-to-face method.

This report details a further investigation into the characteristic frequency response of the transducers over the frequency range of 0 - 50 MHz. Examination is conducted into the transmission of ultrasonic acoustic pulses into water and the detection of these pulses upon reflection from a solid object in what is termed the pulse-echo mode.

Ultrasonic NDT

The application of ultrasound in diverse fields is quite common nowadays. Applications range from flaw detection in materials by the use of non-destructive techniques (NDT), to the imaging of internal organs during medical investigations, to topographical visualisation of surfaces within an acoustically transmitting medium. The above applications all use the principle of generation of a pulse of ultrasound and the subsequent detection of the same pulse upon reflection by an impedance interface within the body under test. Other applications of ultrasound are the use of continuous waves and the principle of Doppler shift for the detection of flow of material within a body and the generation of higher energy ultrasound for medical treatment.

The principle of the pulse-echo mode of NDT or medical imaging techniques works on the detection of the reflected pulse from an interface within the test body. The time taken to detect the reflected pulse after generation by the transmitting transducer gives the distance away from the transducer of the interface if the speed of the ultrasound is known. The distance d is given by

$$d = ct/2 \qquad \ldots(1)$$

where c is the velocity of the ultrasonic pulse, which could be frequency dependent, within the body and t is the time delay between generation and detection of the pulse.

For most pulse-echo systems the ultrasonic pulse is designed to produce the required result. For resolving the time of arrival of a number of reflections occurring at comparable times a short pulse is required. Time domain analysis requires a short pulse for high resolution. If frequency analysis is employed then a

broad bandwidth pulse is required. Although there is a connection between the duration of the pulse and the bandwidth these parameters are not the same.

Short pulses can be achieved by using higher frequencies or by increasing the pulse decay rate. The use of higher frequencies presents a problem of higher attenuation as the attenuation of the ultrasonic wave is frequency dependent. Increasing the decay rate has wasteful side effects of high absorption of ultrasonic energy by the probe.

Experimental

All measurements were performed in a glass tank containing filtered and de-ionised water. The tank measured 130cm long, 70cm wide and 45cm deep. The dimensions of the tank were made large enough so that reflections from the sides of the tank would not interfere with the measurements. If the signals produced are of sufficiently short duration then any unwanted reflections can easily be distinguished due to their longer propagation times. Alternatively, if the source possesses narrow directivity characteristics then the reflections from the sides of the tank will have low amplitudes because they arise from the side lobes of the field distribution. Since all the transducers were excited using the commercial pulser, any unwanted echoes superimposed on the main signal did not pose any erroneous results.

Water filtration was provided by a Fistreem™ System XD-250 de-ioniser which could provide clean and trouble free water at up to 2 litres/minute. Purity as high as 10 MΩ/cm resistivity (0.1 μS/cm conductivity) was achievable. Degassing and temperature control of the water was not available and measurements were made at room temperature (~22°C).

A broad band polymer needle hydrophone constructed from PVDF (The Danish Institute of Biomedical Engineering, Serial No. 1282) having a 1mm diameter active area was used to provide a representation of the pressure field at a given point. Calibration of the hydrophone at 24°C reveals a characteristic narrow peak at approximately 2 MHz but beyond this frequency the sensitivity of the probe may be assumed constant for all practical measurements.

A Gould 4050 Digital Storage Oscilloscope (DSO) was used to acquire the data from the hydrophone or transducer. The DSO was capable of sampling the data at 100 MHz. The input impedance of the DSO is specified at 1 MΩ in parallel with 28 pF. Interface to a PC was enabled by a GPIB IEEE-488 connection which enabled the DSO to be controlled remotely (see figure 1). A computer program written in C language was used to control the DSO to capture, store and download to disc the acquired data. A trigger for the DSO was provided by the pulser unit. The trigger output of the pulser was fed through a delay line so as to trigger the scope at the appropriate time. The delay was produced by an Intercontinental Instruments Inc. Pulse Generator Model PG-2 which allowed a variable delay to be set.

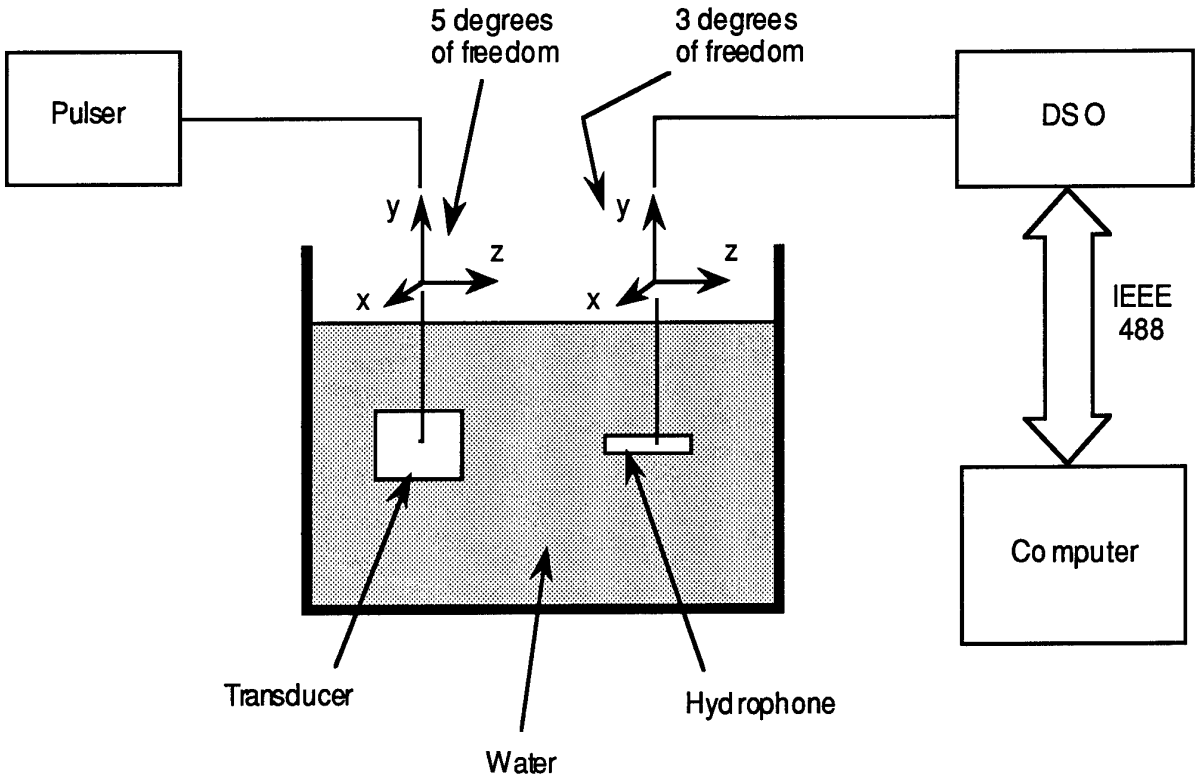

Figure 1: Schematic diagram of water tank with transducer and hydrophone set-up.

Electrical stimulation of the transducers was performed by an ultrasonic pulser/receiver [Par Scientific Instruments SPIKE 150 PR] which produced a spike of rise time 90ns, decay time of 190ns with total duration of 280ns. The generator produces a high voltage spike by the sudden discharge of a capacitor previously charged to several hundreds of volts. This shock excitation is normally used for the stimulation of low-Q polymeric transducers because of their inherently larger bandwidths.

Transducers

Transducers suitable for surface mounted acoustic emission detection or ultrasonic transmission/reception were fabricated from thin films of composite materials. The fabrication method used for these transducers was described in the eighth interim report. This report details the results of investigation into a number of transducers made from various compositions of PTCa and a polymer. The details of the various transducers are summarised in table 1.

Backing material used for the transducers was constructed from an epoxy and tungsten powder composite. The characteristic acoustic impedance of the electroactive film was determined by measurement of the electrical impedance over

the frequency range of 0 - 50MHz. The composition of the epoxy and tungsten composite used for the backing material determines the acoustic impedance of the material. The backing material was constructed to possess the same acoustic impedance as the electroactive film, to provide a backing material which would not create an interface with the film. Any reflection of the acoustic wave from the backing material will produce a 'ringing' effect and extend the acoustic pulse. A transducer with a backing material possessing the same acoustic impedance as that of the piezoelectric material will allow all the sound wave to propagate into the backing material with no reflection at the interface. This correct matching of the acoustic impedance's should result in a pulse produced from the expansion of the front face and its subsequent contraction. In practice an exact match of acoustic impedances is difficult to achieve.

The front face of the transducers were coated with an electrically conducting film. This film was kept as thin as possible so as not to mechanically load the piezoelectric material. It was found that evaporated aluminium was insufficient for this layer in two respects. Firstly the aluminium would be removed by immersion in the water for any extended period of time and secondly the current carrying capabilities of such a thin layer produced an electrical resistance in series with the piezoelectric material. Silver loaded conducting paint was used to provide a conductive layer over the front face of the transducer which was corrosive resistant enough for the experiments.

In this work five different transducers were constructed, three using an electroactive material of PTCa-P(VDF-TrFE) composite and two with PTCa-Epikote composite. Table 1 summaries the properties of the electroactive element of the five transducers.

Label	Material	Thickness [μm]	Za [MRayls]	d_{33} [pC/N]	k_t	f_o [MHz]	Q_m	tanδ	$\tan\delta_m$
T1	PTCa-P(VDF-TrFE) 65vol%/35vol%	193	11.4	32	0.21	5.77	7.95	0.13	0.13
T2	PTCa-P(VDF-TrFE) 65vol%/35vol%	145	11.2	34	0.22	7.53	6.99	0.15	0.13
T3	PTCa-P(VDF-TrFE) 65vol%/35vol%	61	11.8	33	0.21	18.83	6.20	0.16	0.16
T4	PTCa-Epikote 55vol%/45vol%	138	14.4	23	0.23	12.06	11.67	0.06	0.09
T5	PTCa-Epikote 58vol%/42vol%	146	10.7	30	0.19	8.17	9.9	0.04	0.10

Table 1: Acoustic and piezoelectric properties of electroactive elements.

T1 and T2 have been constructed with thicknesses such to produce a resonant frequency in the range <10 MHz. T3 shows a resonant frequency of 18.8 MHz, where as the resonant frequencies of T5 and T4 are 8.17 and 12.06 MHz respectively. The resonant frequencies are determined by the thickness of the electroactive element and by the density of the material.

Results and Discussion

Data acquired from the DSO was downloaded onto a computer for analysis. Data from a single capture of the pulse on the DSO was downloaded onto a computer for analyses. This data comprised of 1024 datum points containing the pulse. The individual sets of data were multiplied by a Hanning window of the same length before a fast Fourier transform (FFT) analysis was performed. The absolute value of the FFT was used to determine the power spectrum estimation of the individual pulse. A total of 99 individual pulses were captured and analysed this way and the average power spectrum density was calculated. This average was then normalised to the peak of the spectrum.

Transmit Mode

In the transmit mode the transducers were held in position by a clamp which could be adjusted in the x, y and z directions (see figure 1) and also rotated about the z-axis and the x-axis. The hydrophone, which could be adjusted in the x, y and z direction, was positioned along the central axis of the ultrasonic beam such that the active area was perpendicular to the axis.

The transducer and hydrophone were aligned so as to produce the maximum signal from the hydrophone. This was achieved by adjustment of the hydrophone position in the x-y plane while sensing the acoustic field close (i.e. < 50mm) to the transducer front face. The rotation and tilt about the y and x axis of the transducer was then adjusted while sensing the acoustic field far (i.e. > 300mm) from the transducer, once the x-y co-ordinates had been fixed.

Measurements were taken at 5cm intervals along the z-axis up to a distance of 30cm from the transducer face. Waveforms of the pulses at a distance of 20cm from the transducer are shown in figures 1 - 6 along with their corresponding FFT spectrums. Bandwidths of the transmitted pulses were calculated from the -3dB level. The maximum amplitude, duration and bandwidths of the measured pulses from the output of the hydrophone can be seen in table 2.

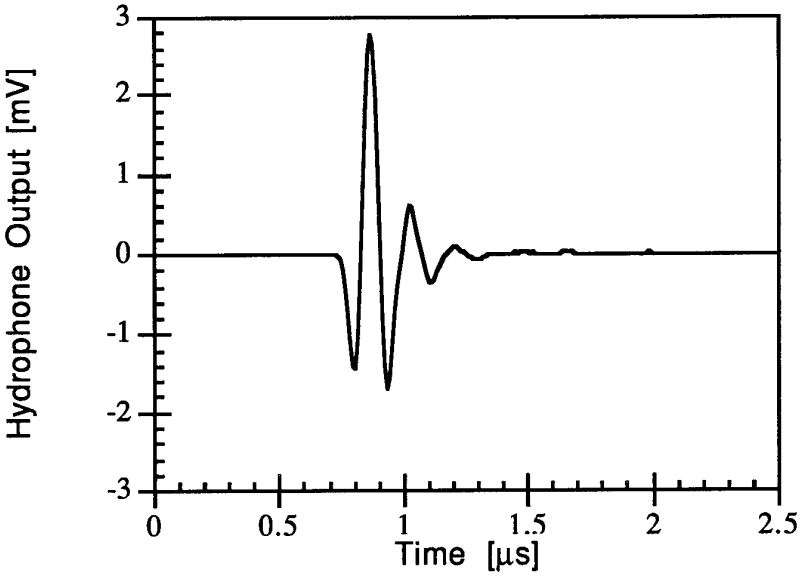

Figure 2(a): Hydrophone output waveform of pulse generated by T1

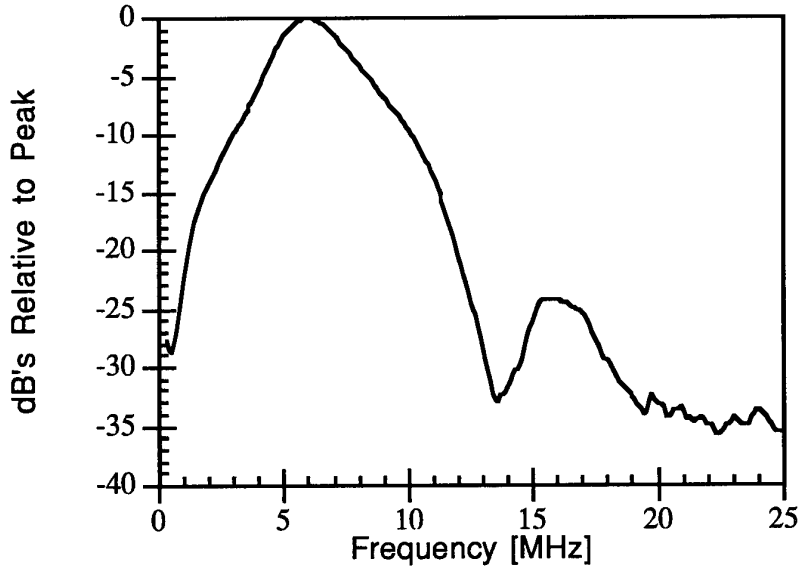

Figure 2(b): FFT spectrum of waveform in figure 2(a).

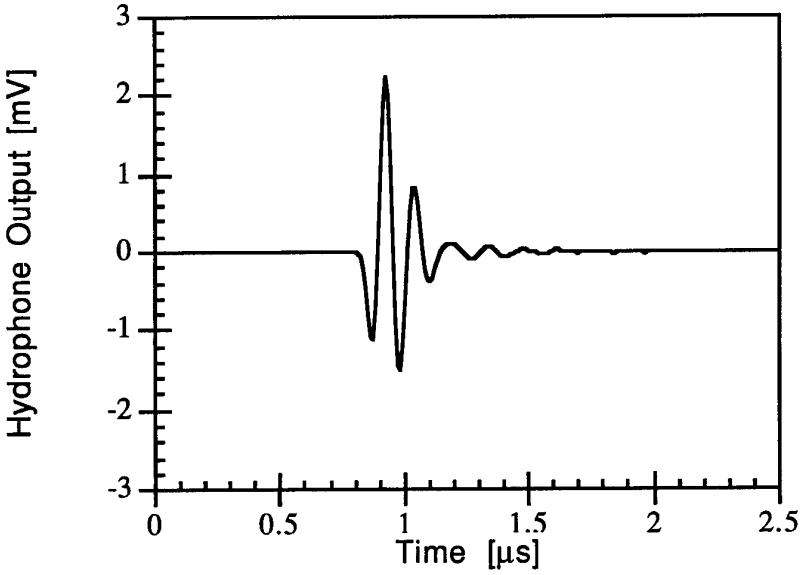

Figure 3(a): Hydrophone output waveform of pulse generated by T2

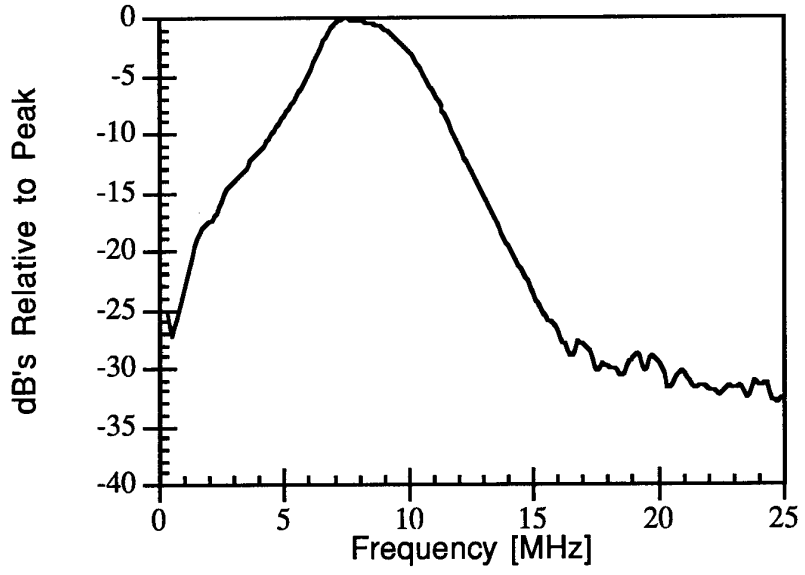

Figure 3(b): FFT spectrum of waveform in figure 3(a).

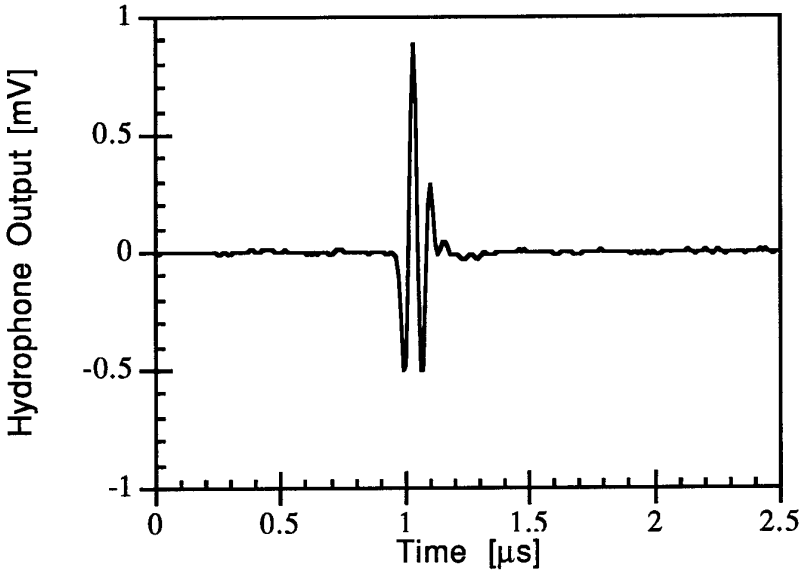

Figure 4(a): Hydrophone output waveform of pulse generated by T3

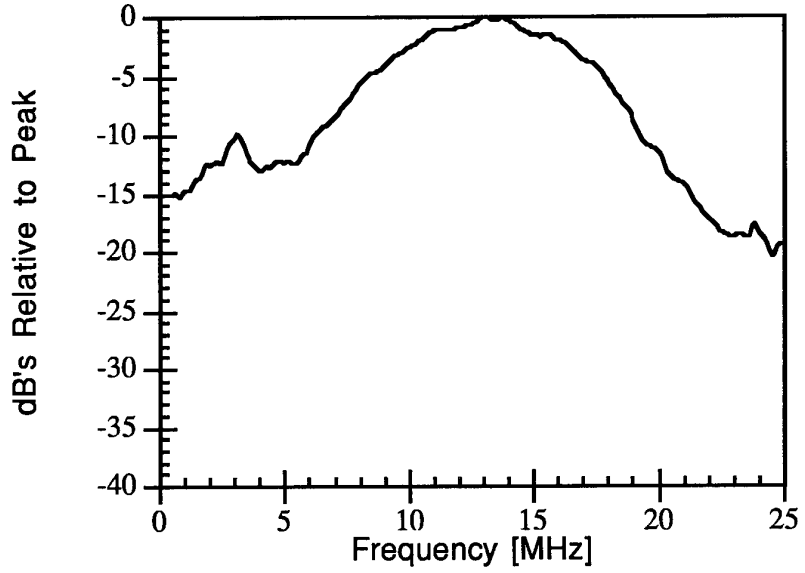

Figure 4(b): FFT spectrum of waveform in figure 4(a).

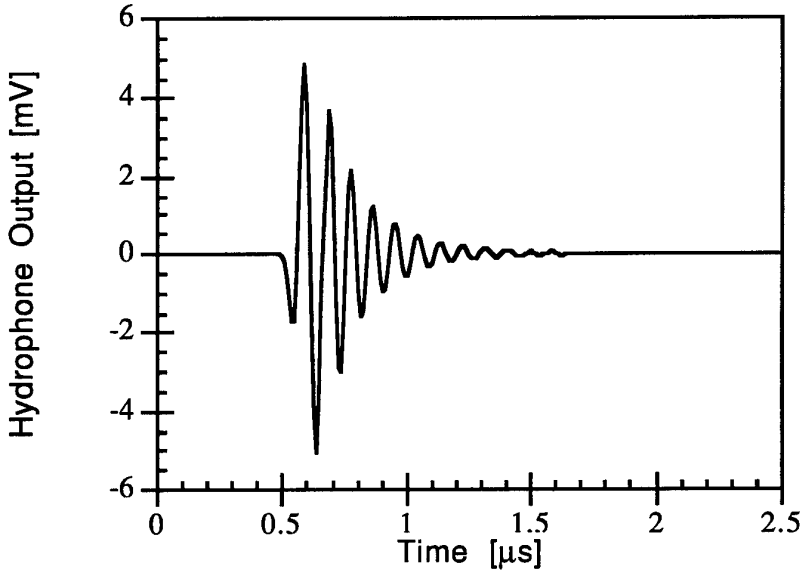

Figure 5(a): Hydrophone output waveform of pulse generated by T4

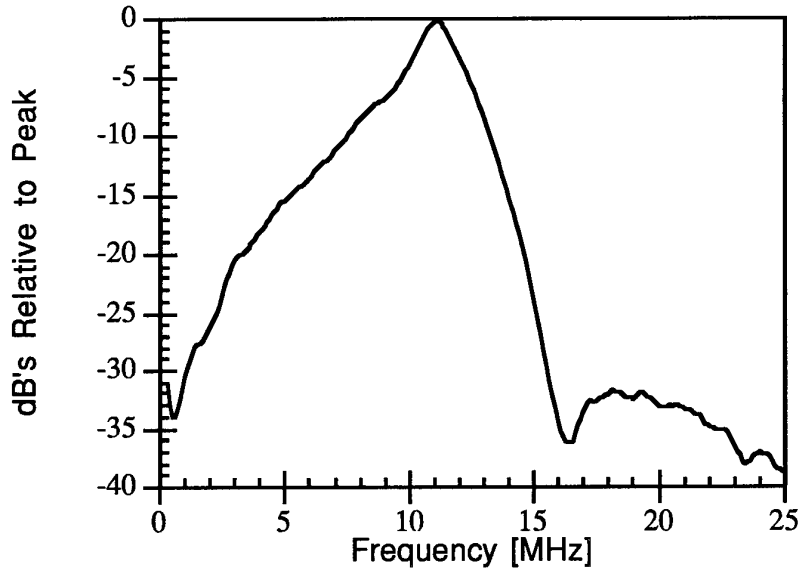

Figure 5(b): FFT spectrum of waveform in figure 5(a).

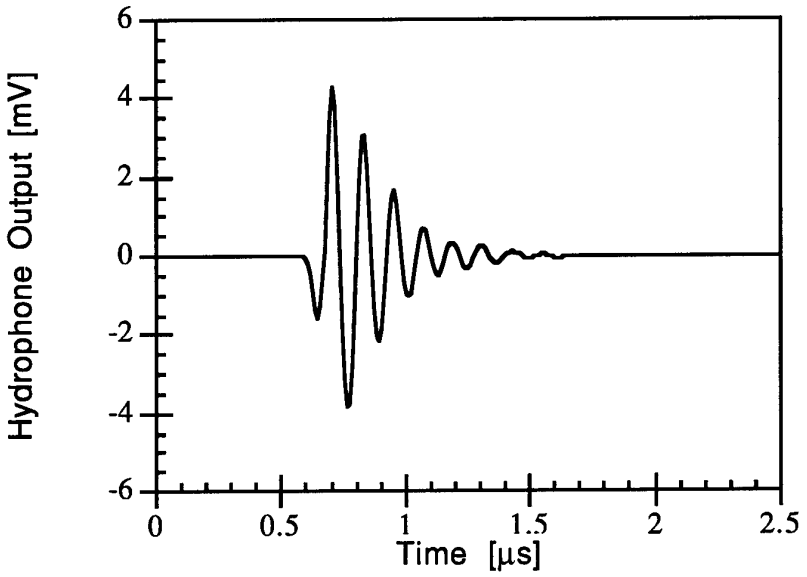

Figure 6(a): Hydrophone output waveform of pulse generated by T5

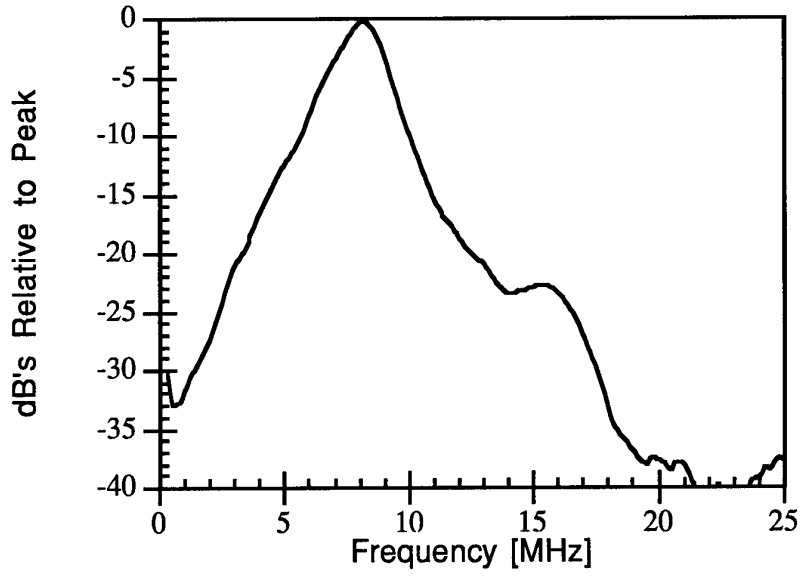

Figure 6(b): FFT spectrum of waveform in figure 6(a).

Transducer	Duration of Pulse [μs]	Centre Frequency [MHz]	-3dB Bandwidth [MHz]	-3dB Bandwidth [%]	Maximum Amplitude of Pulse [mV Peak-Peak]	Gain-BW [MHz-mV]	Gain-BW (%-mV)
T1	0.62	6.06	2.97	48	4.48	13.31	2.15
T2	0.84	8.09	3.72	46	4.15	15.44	1.91
T3	0.30	13.05	6.41	49	0.61	3.91	0.30
T4	1.16	11.07	1.75	16	9.89	17.31	1.58
T5	1.05	8.17	1.82	22	8.19	14.91	1.80

Table 2: Transmit mode characteristics of transducers.

It can be seen from table 2 that the centre frequencies of the transducers, except for T3, follow closely with the resonant frequencies of the freely suspended electroactive element as is expected.

The resonant frequency of the electroactive material of T3 is about 18 MHz where the centre frequency of the transmitted pulse at 20cm from the transducer is approximately 13 MHz. This shift in frequencies may be explained by the higher frequencies being attenuating quicker than the lower frequencies over the distance travelled in water.

From the results displayed in table 2 it can be seen that all the pulses produced by the transducers have broad bandwidth characteristics about the resonant frequencies. Transducer T3 having the largest bandwidth of the transducers constructed from PTCa-P(VDF-TrFE) with the correspondingly higher centre frequency and shorter pulse duration. Transducers T1 and T2 show a corresponding decrease in bandwidth with decreasing centre frequency. A corresponding increase in pulse duration is seen with this decrease in centre frequency although T1 has a shorter pulse duration than T2. This discrepancy is also highlighted when the fractional bandwidth of these transducers are considered, T1 having a higher fractional bandwidth than T2 indicating a transducer with a closer matched backing material. In the spectrum of the transmitted pulse of T1 the contribution from the third harmonic can clearly be seen.

Transducers T4 and T5, constructed from a PTCa-Epoxy composite, show higher peak amplitudes than the transducers constructed from PTCa-P(VDF-TrFE). The duration of the pulses are considerably longer as well which would indicate a lower damped system, thus explaining the increase in acoustic wave amplitude. The centre frequencies of T4 and T5 occur at 11.07 and 8.17 MHz respectively while their bandwidths are comparable at 1.75 and 1.82 MHz respectively. For a transducer with a higher resonant frequency a shorter pulse duration is expected for a properly back transducer. T4 having a higher resonant frequency than T5 but

comparable pulse length indicates a higher impedance mismatch of the backing material or the bond layer with the electroactive film thus reducing the bandwidth of the signal.

The non symmetrical form of the FFT spectrums of T4 and T5 are indicative of reflections occurring at the bond interface between the piezoelectric material and the backing material. Silk [1] suggests that the backing material (i.e.. tungsten and epoxy composite) although does effect the shape of the pulse, does not appear to be the major source of transducer variation. The converse is true for the bond layer which causes the main variation in transducer performance. The prolonged ringing of T4 and T5 can be put down to inefficient bond layers.

Receive Mode

In the receive mode, the pulses generated by the transducers are reflected by an aluminium plate placed at a distance D from the front face of the transducer, where D is greater than the transducers near-field/far-field interface. The far-field is the region in which the acoustic energy flow proceeds essentially as though coming from a point source located in the vicinity of the transducer assembly. For an unfocused transducer, like the ones in this study, the near-field/far-field interface is commonly at a distance such that

$$D \geq \frac{S}{\pi\lambda} \qquad \ldots(2)$$

where S is the radiating cross sectional area and λ is the acoustic wavelength of the medium. The returning echo is subsequently detected by the same transducer. The commercial pulser (PAR 150PR) has capabilities of detecting and outputting an analogue representation of the signal from the transducer. The signal is later scaled after detection by the oscilloscope to represent truthfully the output from the transducer.

The measured pulses and their corresponding FFT spectrums are shown in figures 7 - 11 for the respective transducers. The aluminium plate was placed a distance of 20cm from the front face of the transducer which provides a distance greater than the near-field/far-field interface distance for T1, T2, T4 and T5. This distance fails to meet this criteria for T3, but it was found that the amplitude of the transmitted pulse from this transducer was attenuated too severely over a distance of 40cm (transmitted and reflected journey) to be easily detected by the transducer. The reflected pulse in figure 9(a) and it's corresponding FFT spectrum correspond to a reflection from an aluminium plate placed at a distance of 10cm along the beam axis from the transducer's front face. The characteristics of the waveforms and spectrums are summarised in table 3.

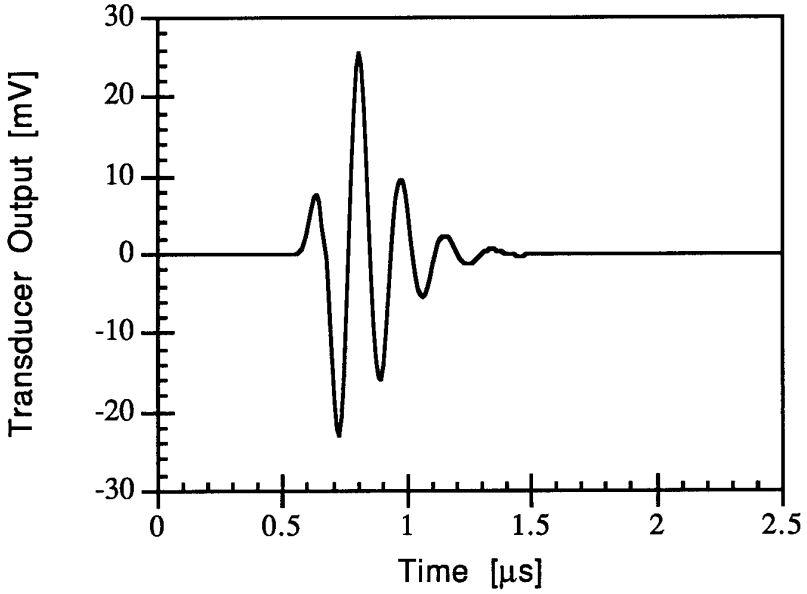

Figure 7(a): Transducer output waveform of pulse detected by T1

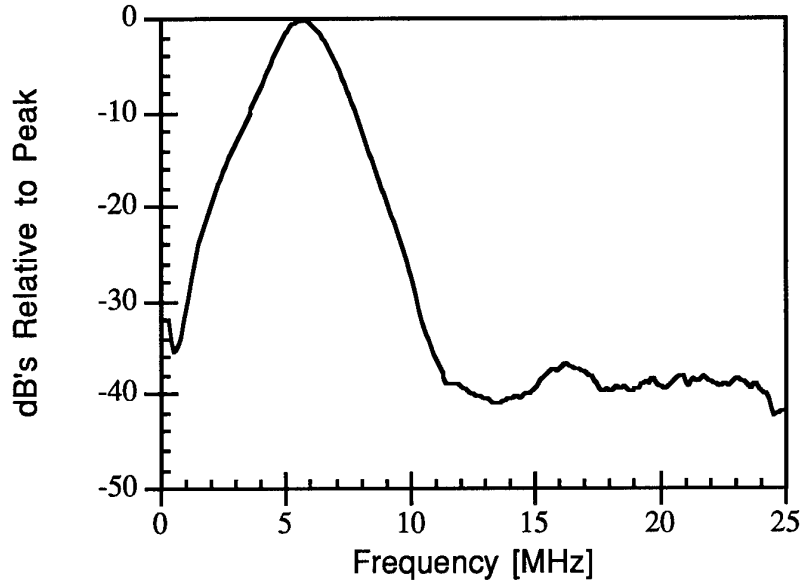

Figure 7(b): FFT spectrum of waveform in figure 7(a).

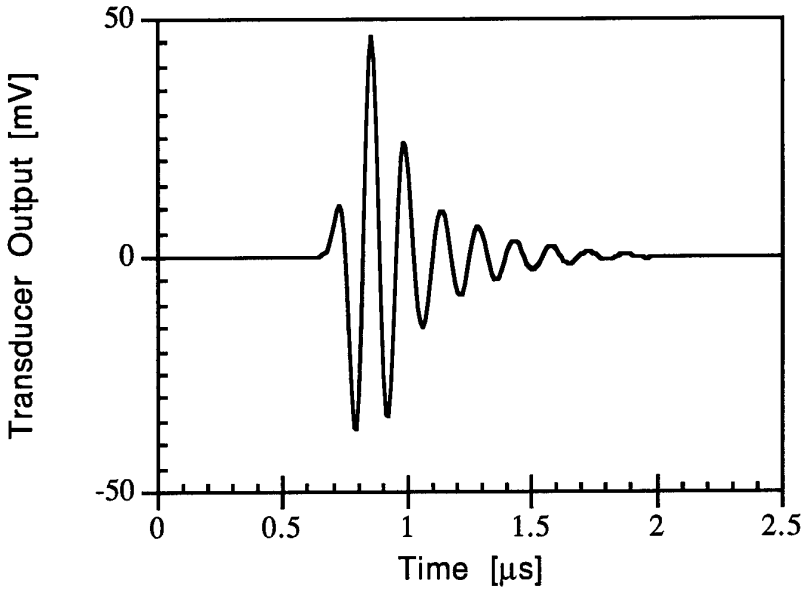

Figure 8(a): Transducer output waveform of pulse detected by T2

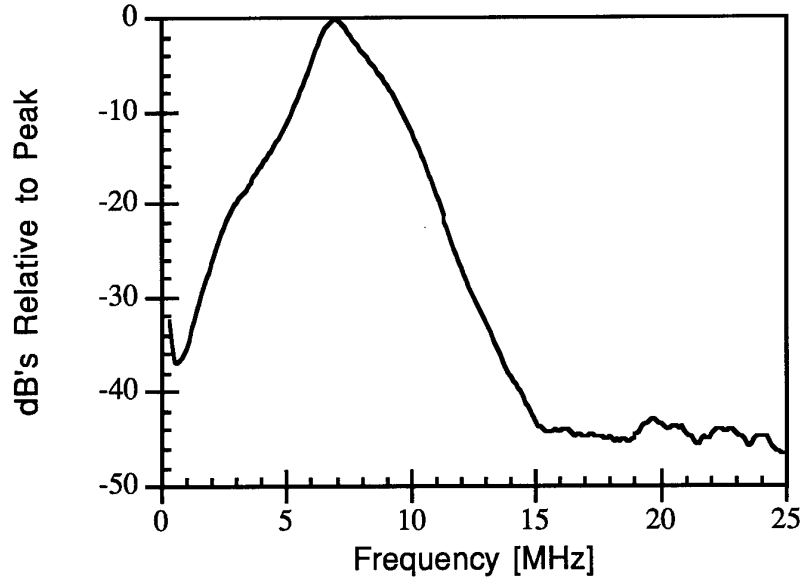

Figure 8(b): FFT spectrum of waveform in figure 8(a).

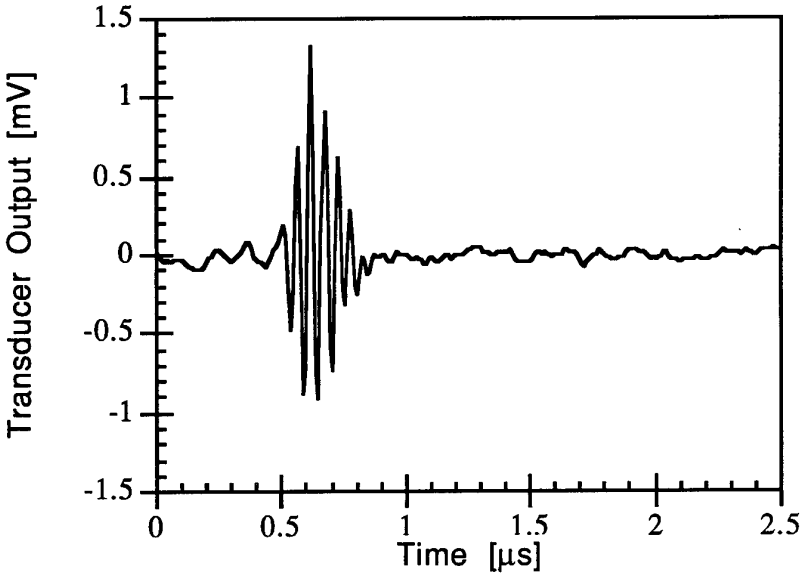

Figure 9(a): Transducer output waveform of pulse detected by T3

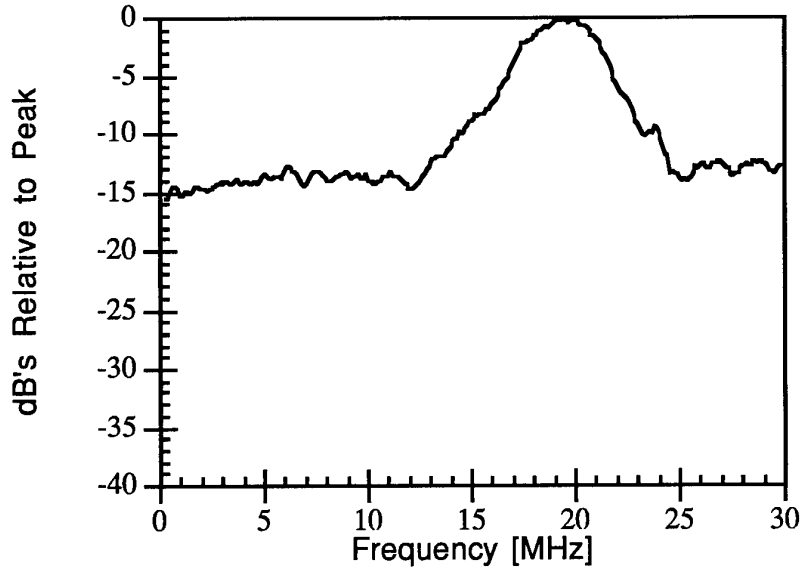

Figure 9(b): FFT spectrum of waveform in figure 9(a).

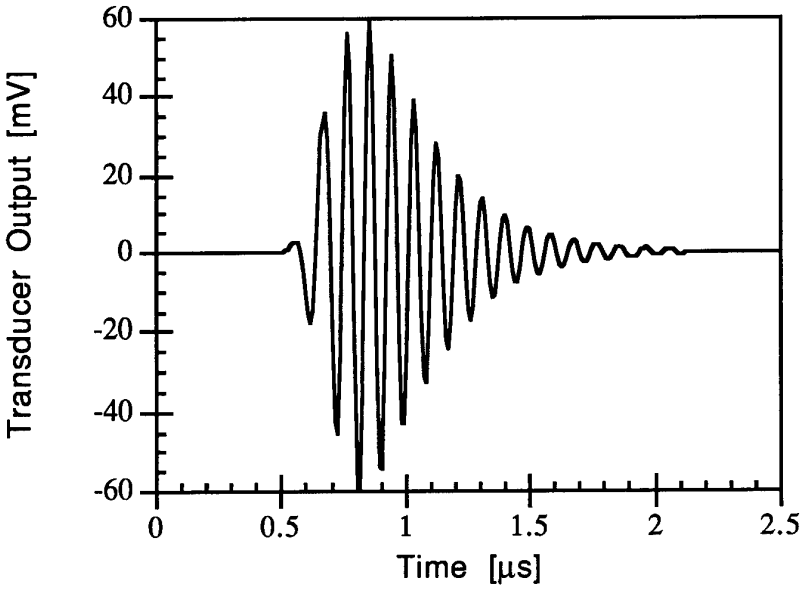

Figure 10(a): Transducer output waveform of pulse detected by T4

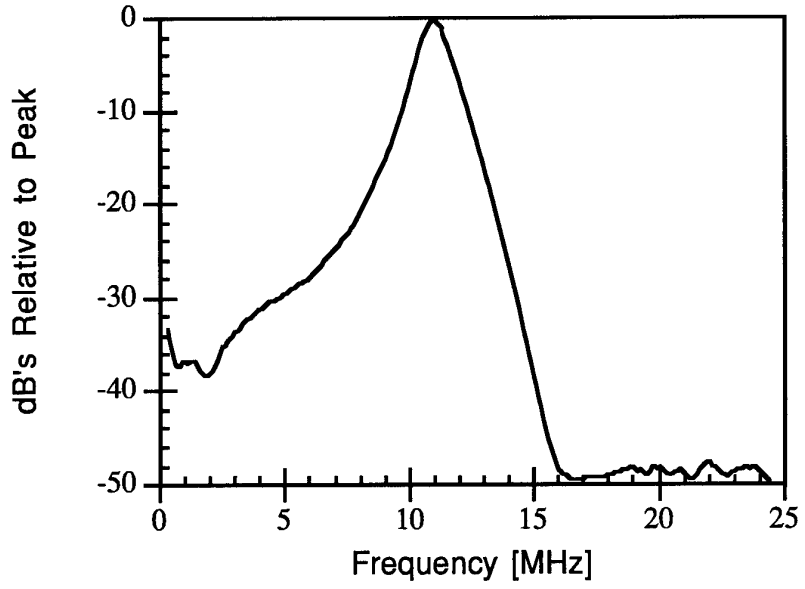

Figure 10(b): FFT spectrum of waveform in figure 10(a).

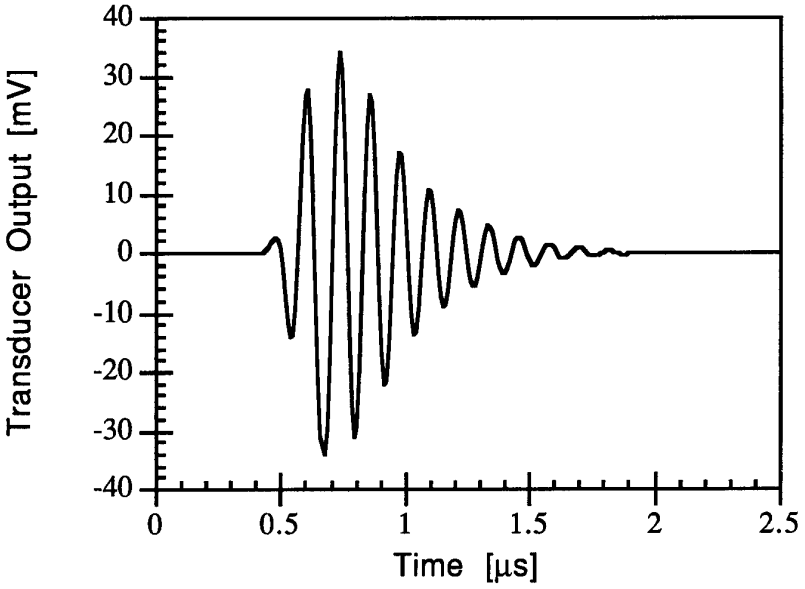

Figure 11(a): Transducer output waveform of pulse detected by T5

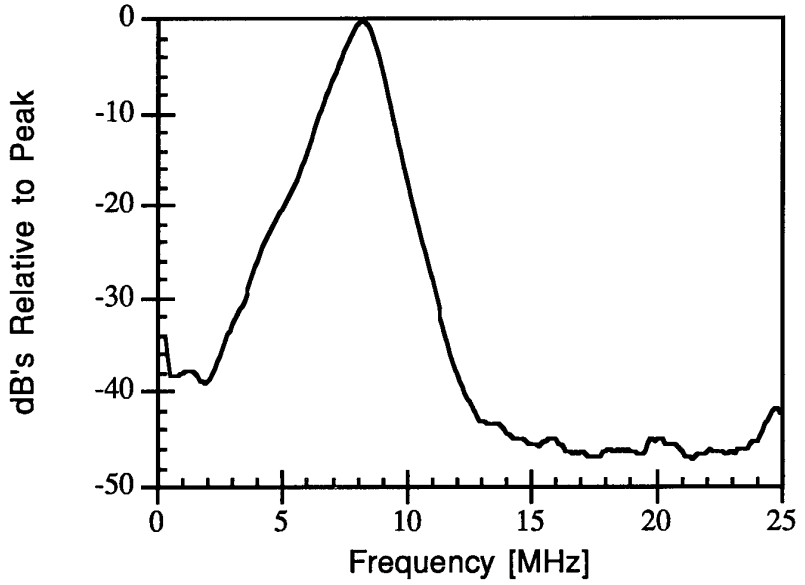

Figure 11(b): FFT spectrum of waveform in figure 11(a).

Transducer	Duration of Pulse [μs]	Centre Frequency [MHz]	-3dB Bandwidth [MHz]	-3dB Bandwidth [%]	Maximum Amplitude of Pulse [mV peak-peak]	Gain-BW [MHz-mV]	Gain-BW (%-mV)
T1	0.91	5.66	1.97	35	48.64	95.82	17.02
T2	1.20	7.14	1.55	22	83.00	128.65	18.26
T3*	0.43*	19.52*	3.52*	18*	2.22*	7.81*	0.40*
T4	1.55	11.05	1.21	11	118.58	143.48	13.04
T5	1.42	8.13	1.24	15	67.99	84.31	10.20

Table 3: Receive mode characteristics of transducers. * Measured pulse of T3 was reflected from an aluminium plate 10cm from the front face of the transducer.

From table 3 it can be seen that the amplitude values associated with the pulses are far greater than the measured transmitted values. This is partly due to the fact that the transducers are more sensitive than the hydrophone due to a larger detecting area thus providing a larger output signal. The duration of the pulses are also longer, this is possibly due to the extra sensitivity of the detector, however this fact has yet to be proved. The lengthening of the pulse has a contributing effect to the shortening of the bandwidth.

The FFT spectrum, corresponding to the output from transducer T4, displays the characteristic non-symmetrical appearance due to a thick or patchy bond line as seen in the transmitted pulse. This could explain the high output seen from T4 due to the low damping of the acoustic energy.

The transducer T3 shows a low output due to the high attenuation of the high frequency pulse. The centre frequency to the detected pulse appears at 19.5 MHz which is close to the resonant frequency of the unclamped electroactive material. The higher frequencies have appeared to be detected with greater sensitivity than the lower ones. The discrepancy in the centre frequencies of the transmitted and detected pulses may be due to the sensitivity of the hydrophone diminishing at high frequencies but at the present moment this shift in frequencies is not fully understood.

Conclusion

When considering the gain-bandwidth products which have been computed by multiplying the peak to peak amplitudes with the bandwidths, it appears that the transducers constructed from PTCa-P(VDF-TrFE) are more efficient for producing and detecting high amplitude, broad bandwidth pulses than transducers

constructed from PTCa-Epikote composites. Earlier work [2] with composites has found that the PTCa-Epikote composite should be approximately 64% more efficient as a transducer receiver material than the PTCa-P(VDF-TrFE) composite. This may be accomplished with proper backing of the electroactive material provided the material has been efficiently poled.

Further Work

Further work is in progress to investigate the transducers constructed from PTCa-Epikote composites. Their characteristic frequency response in the range 0 - 1 MHz will be studied using the face-to-face method of calibration together with their performance in the acoustic emission detection mode. This work will be conducted on embedded thin films of PTCa-Epikote composites in fibre reinforced laminates and transducers suitable for surface mounted acoustic emission detectors constructed from this material.

Although not included in the contract proposal but of interest with respect to transducers, suggestions for further work would concern the theoretical modelling of the electrical and mechanical properties of these transducers. In order to simulate the behaviour of the thickness mode ultrasonic transducers various types of analysis have been proposed which can be classified into frequency or time domain methods. Frequency domain methods such as Mason's model [3] consist of an electrical analogue which behaves in the frequency domain as the piezoelectric transducer. Time domain methods include a systems approach based on z-transforms proposed by Hayward [4] and the simulation on a computer of the time behaviour of ultrasonic transducers using a SPICE program [5]. The use of ABCD matrices are also commonly applicable to two-port networks which are used to represent ultrasonic transducers [6].

References

1. Silk, M.G., *Ultrasonic Transducers for Nondestructive Testing*. A.E. Bailey. 1984, UK: Adam Hilger Ltd., Techno House, Redcliffe Way, Bristol, BS1 6NX. 10.

2. Dias, C., M.P. Wenger, P. Blanas, R.J. Shuford, Y. Hinton, and D.K. Das-Gupta. *Intelligent Piezoelectric Composite Materials for Sensors*. in *2nd International Conference on Intelligent Materials*. 1994. Williamsburg, VA, USA:

3. Mason, W.P., *Electromechanical Transducers and Wave Filters*. 2 ed. 1948, New York, U.S.A.: D. Van Nostrand Co.

4. Hayward, G. and M. Jackson, *Discrete time modelling of the thickness mode piezoelectric transducer*. IEEE Trans. Sonics and Ultrasonics, 1984. **SU-31**(3).

5. Morris, S.A. and C.G. Hutchens, *Implementation of Mason's model on circuit analysis programs.* IEEE Trans. Ultrasonics, Ferroelectrics and Freq. Control, 1986. **UFFC-33**(3): p. 295 - 298.

6. Dias, C., D.K. Das-Gupta, Y. Hinton, and R.J. Shuford, *Polymer/Ceramic Composites for Piezoelectric Sensors.* Sensors and Actuators A, 1993. **37-38**: pp. 343 - 347.